Measurement of the Angular Distribution of Electrons from $W \to e\nu$ Decays Observed in $p\bar{p}$ Collisions at $\sqrt{s} = 1.8$ TeV

The DØ Collaboration *

Fermi National Accelerator Laboratory, Batavia, Illinois 60510

(June 14, 1999)

Abstract

We present a preliminary measurement of the electron angular distribution parameter α_2 in $W \to e\nu$ events using data collected by the DØ detector during the 1994–1995 Tevatron run. We compare our results with next-to-leading order perturbative QCD, which predicts an angular distribution of $(1 \pm \alpha_1 \cos\theta^* + \alpha_2 \cos^2\theta^*)$, where θ^* is the angle between the charged lepton and the antiproton in the Collins-Soper frame. In the presence of QCD corrections, the parameters α_1 and α_2 become functions of p_T^W, the W boson transverse momentum. We present the first measurement of α_2 as a function of p_T^W. This measurement is of importance, because it provides a test of next-to-leading order QCD corrections which are a non-negligible contribution to the W mass measurement.

*Submitted to the *International Europhysics Conference* on *High Energy Physics*, *EPS-HEP99*, 15 – 21 July, 1999, Tampere, Finland.

B. Abbott,[45] M. Abolins,[42] V. Abramov,[18] B.S. Acharya,[11] I. Adam,[44] D.L. Adams,[54] M. Adams,[28] S. Ahn,[27] V. Akimov,[16] G.A. Alves,[2] N. Amos,[41] E.W. Anderson,[34] M.M. Baarmand,[47] V.V. Babintsev,[18] L. Babukhadia,[20] A. Baden,[38] B. Baldin,[27] S. Banerjee,[11] J. Bantly,[51] E. Barberis,[21] P. Baringer,[35] J.F. Bartlett,[27] A. Belyaev,[17] S.B. Beri,[9] I. Bertram,[19] V.A. Bezzubov,[18] P.C. Bhat,[27] V. Bhatnagar,[9] M. Bhattacharjee,[47] G. Blazey,[29] S. Blessing,[25] P. Bloom,[22] A. Boehnlein,[27] N.I. Bojko,[18] F. Borcherding,[27] C. Boswell,[24] A. Brandt,[27] R. Breedon,[22] G. Briskin,[51] R. Brock,[42] A. Bross,[27] D. Buchholz,[30] V.S. Burtovoi,[18] J.M. Butler,[39] W. Carvalho,[2] D. Casey,[42] Z. Casilum,[47] H. Castilla-Valdez,[14] D. Chakraborty,[47] S.V. Chekulaev,[18] W. Chen,[47] S. Choi,[13] S. Chopra,[25] B.C. Choudhary,[24] J.H. Christenson,[27] M. Chung,[28] D. Claes,[43] A.R. Clark,[21] W.G. Cobau,[38] J. Cochran,[24] L. Coney,[32] W.E. Cooper,[27] D. Coppage,[35] C. Cretsinger,[46] D. Cullen-Vidal,[51] M.A.C. Cummings,[29] D. Cutts,[51] O.I. Dahl,[21] K. Davis,[20] K. De,[52] K. Del Signore,[41] M. Demarteau,[27] D. Denisov,[27] S.P. Denisov,[18] H.T. Diehl,[27] M. Diesburg,[27] G. Di Loreto,[42] P. Draper,[52] Y. Ducros,[8] L.V. Dudko,[17] S.R. Dugad,[11] A. Dyshkant,[18] D. Edmunds,[42] J. Ellison,[24] V.D. Elvira,[47] R. Engelmann,[47] S. Eno,[38] G. Eppley,[54] P. Ermolov,[17] O.V. Eroshin,[18] H. Evans,[44] V.N. Evdokimov,[18] T. Fahland,[23] M.K. Fatyga,[46] S. Feher,[27] D. Fein,[20] T. Ferbel,[46] H.E. Fisk,[27] Y. Fisyak,[48] E. Flattum,[27] G.E. Forden,[20] M. Fortner,[29] K.C. Frame,[42] S. Fuess,[27] E. Gallas,[27] A.N. Galyaev,[18] P. Gartung,[24] V. Gavrilov,[16] T.L. Geld,[42] R.J. Genik II,[42] K. Genser,[27] C.E. Gerber,[27] Y. Gershtein,[51] B. Gibbard,[48] B. Gobbi,[30] B. Gómez,[5] G. Gómez,[38] P.I. Goncharov,[18] J.L. González Solís,[14] H. Gordon,[48] L.T. Goss,[53] K. Gounder,[24] A. Goussiou,[47] N. Graf,[48] P.D. Grannis,[47] D.R. Green,[27] J.A. Green,[34] H. Greenlee,[27] S. Grinstein,[1] P. Grudberg,[21] S. Grünendahl,[27] G. Guglielmo,[50] J.A. Guida,[20] J.M. Guida,[51] A. Gupta,[11] S.N. Gurzhiev,[18] G. Gutierrez,[27] P. Gutierrez,[50] N.J. Hadley,[38] H. Haggerty,[27] S. Hagopian,[25] V. Hagopian,[25] K.S. Hahn,[46] R.E. Hall,[23] P. Hanlet,[40] S. Hansen,[27] J.M. Hauptman,[34] C. Hays,[44] C. Hebert,[35] D. Hedin,[29] A.P. Heinson,[24] U. Heintz,[39] R. Hernández-Montoya,[14] T. Heuring,[25] R. Hirosky,[28] J.D. Hobbs,[47] B. Hoeneisen,[6] J.S. Hoftun,[51] F. Hsieh,[41] Tong Hu,[31] A.S. Ito,[27] S.A. Jerger,[42] R. Jesik,[31] T. Joffe-Minor,[30] K. Johns,[20] M. Johnson,[27] A. Jonckheere,[27] M. Jones,[26] H. Jöstlein,[27] S.Y. Jun,[30] C.K. Jung,[47] S. Kahn,[48] D. Karmanov,[17] D. Karmgard,[25] R. Kehoe,[32] S.K. Kim,[13] B. Klima,[27] C. Klopfenstein,[22] B. Knuteson,[21] W. Ko,[22] J.M. Kohli,[9] D. Koltick,[33] A.V. Kostritskiy,[18] J. Kotcher,[48] A.V. Kotwal,[44] A.V. Kozelov,[18] E.A. Kozlovsky,[18] J. Krane,[34] M.R. Krishnaswamy,[11] S. Krzywdzinski,[27] M. Kubantsev,[36] S. Kuleshov,[16] Y. Kulik,[47] S. Kunori,[38] F. Landry,[42] G. Landsberg,[51] A. Leflat,[17] J. Li,[52] Q.Z. Li,[27] J.G.R. Lima,[3] D. Lincoln,[27] S.L. Linn,[25] J. Linnemann,[42] R. Lipton,[27] A. Lucotte,[47] L. Lueking,[27] A.K.A. Maciel,[29] R.J. Madaras,[21] R. Madden,[25] L. Magaña-Mendoza,[14] V. Manankov,[17] S. Mani,[22] H.S. Mao,[4] R. Markeloff,[29] T. Marshall,[31] M.I. Martin,[27] R.D. Martin,[28] K.M. Mauritz,[34] B. May,[30] A.A. Mayorov,[18] R. McCarthy,[47] J. McDonald,[25] T. McKibben,[28] J. McKinley,[42] T. McMahon,[49] H.L. Melanson,[27] M. Merkin,[17] K.W. Merritt,[27] C. Miao,[51] H. Miettinen,[54] A. Mincer,[45] C.S. Mishra,[27] N. Mokhov,[27] N.K. Mondal,[11] H.E. Montgomery,[27] M. Mostafa,[1] H. da Motta,[2] C. Murphy,[28] F. Nang,[20] M. Narain,[39] V.S. Narasimham,[11] A. Narayanan,[20] H.A. Neal,[41] J.P. Negret,[5] P. Nemethy,[45] D. Norman,[53] L. Oesch,[41] V. Oguri,[3] N. Oshima,[27] D. Owen,[42] P. Padley,[54] A. Para,[27] N. Parashar,[40] Y.M. Park,[12] R. Partridge,[51] N. Parua,[7] M. Paterno,[46] B. Pawlik,[15] J. Perkins,[52] M. Peters,[26] R. Piegaia,[1] H. Piekarz,[25]

Y. Pischalnikov,[33] B.G. Pope,[42] H.B. Prosper,[25] S. Protopopescu,[48] J. Qian,[41]
P.Z. Quintas,[27] R. Raja,[27] S. Rajagopalan,[48] O. Ramirez,[28] N.W. Reay,[36] S. Reucroft,[40]
M. Rijssenbeek,[47] T. Rockwell,[42] M. Roco,[27] P. Rubinov,[30] R. Ruchti,[32] J. Rutherfoord,[20]
A. Sánchez-Hernández,[14] A. Santoro,[2] L. Sawyer,[37] R.D. Schamberger,[47] H. Schellman,[30]
J. Sculli,[45] E. Shabalina,[17] C. Shaffer,[25] H.C. Shankar,[11] R.K. Shivpuri,[10] D. Shpakov,[47]
M. Shupe,[20] R.A. Sidwell,[36] H. Singh,[24] J.B. Singh,[9] V. Sirotenko,[29] E. Smith,[50]
R.P. Smith,[27] R. Snihur,[30] G.R. Snow,[43] J. Snow,[49] S. Snyder,[48] J. Solomon,[28]
M. Sosebee,[52] N. Sotnikova,[17] M. Souza,[2] N.R. Stanton,[36] G. Steinbrück,[50]
R.W. Stephens,[52] M.L. Stevenson,[21] F. Stichelbaut,[48] D. Stoker,[23] V. Stolin,[16]
D.A. Stoyanova,[18] M. Strauss,[50] K. Streets,[45] M. Strovink,[21] A. Sznajder,[2] P. Tamburello,[38]
J. Tarazi,[23] M. Tartaglia,[27] T.L.T. Thomas,[30] J. Thompson,[38] D. Toback,[38] T.G. Trippe,[21]
P.M. Tuts,[44] V. Vaniev,[18] N. Varelas,[28] E.W. Varnes,[21] A.A. Volkov,[18] A.P. Vorobiev,[18]
H.D. Wahl,[25] J. Warchol,[32] G. Watts,[51] M. Wayne,[32] H. Weerts,[42] A. White,[52]
J.T. White,[53] J.A. Wightman,[34] S. Willis,[29] S.J. Wimpenny,[24] J.V.D. Wirjawan,[53]
J. Womersley,[27] D.R. Wood,[40] R. Yamada,[27] P. Yamin,[48] T. Yasuda,[27] P. Yepes,[54] K. Yip,[27]
C. Yoshikawa,[26] S. Youssef,[25] J. Yu,[27] Y. Yu,[13] Z. Zhou,[34] Z.H. Zhu,[46] M. Zielinski,[46]
D. Zieminska,[31] A. Zieminski,[31] V. Zutshi,[46] E.G. Zverev,[17] and A. Zylberstejn[8]

(DØ Collaboration)

[1]Universidad de Buenos Aires, Buenos Aires, Argentina
[2]LAFEX, Centro Brasileiro de Pesquisas Físicas, Rio de Janeiro, Brazil
[3]Universidade do Estado do Rio de Janeiro, Rio de Janeiro, Brazil
[4]Institute of High Energy Physics, Beijing, People's Republic of China
[5]Universidad de los Andes, Bogotá, Colombia
[6]Universidad San Francisco de Quito, Quito, Ecuador
[7]Institut des Sciences Nucléaires, IN2P3-CNRS, Universite de Grenoble 1, Grenoble, France
[8]DAPNIA/Service de Physique des Particules, CEA, Saclay, France
[9]Panjab University, Chandigarh, India
[10]Delhi University, Delhi, India
[11]Tata Institute of Fundamental Research, Mumbai, India
[12]Kyungsung University, Pusan, Korea
[13]Seoul National University, Seoul, Korea
[14]CINVESTAV, Mexico City, Mexico
[15]Institute of Nuclear Physics, Kraków, Poland
[16]Institute for Theoretical and Experimental Physics, Moscow, Russia
[17]Moscow State University, Moscow, Russia
[18]Institute for High Energy Physics, Protvino, Russia
[19]Lancaster University, Lancaster, United Kingdom
[20]University of Arizona, Tucson, Arizona 85721
[21]Lawrence Berkeley National Laboratory and University of California, Berkeley, California 94720
[22]University of California, Davis, California 95616
[23]University of California, Irvine, California 92697
[24]University of California, Riverside, California 92521
[25]Florida State University, Tallahassee, Florida 32306

[26]University of Hawaii, Honolulu, Hawaii 96822
[27]Fermi National Accelerator Laboratory, Batavia, Illinois 60510
[28]University of Illinois at Chicago, Chicago, Illinois 60607
[29]Northern Illinois University, DeKalb, Illinois 60115
[30]Northwestern University, Evanston, Illinois 60208
[31]Indiana University, Bloomington, Indiana 47405
[32]University of Notre Dame, Notre Dame, Indiana 46556
[33]Purdue University, West Lafayette, Indiana 47907
[34]Iowa State University, Ames, Iowa 50011
[35]University of Kansas, Lawrence, Kansas 66045
[36]Kansas State University, Manhattan, Kansas 66506
[37]Louisiana Tech University, Ruston, Louisiana 71272
[38]University of Maryland, College Park, Maryland 20742
[39]Boston University, Boston, Massachusetts 02215
[40]Northeastern University, Boston, Massachusetts 02115
[41]University of Michigan, Ann Arbor, Michigan 48109
[42]Michigan State University, East Lansing, Michigan 48824
[43]University of Nebraska, Lincoln, Nebraska 68588
[44]Columbia University, New York, New York 10027
[45]New York University, New York, New York 10003
[46]University of Rochester, Rochester, New York 14627
[47]State University of New York, Stony Brook, New York 11794
[48]Brookhaven National Laboratory, Upton, New York 11973
[49]Langston University, Langston, Oklahoma 73050
[50]University of Oklahoma, Norman, Oklahoma 73019
[51]Brown University, Providence, Rhode Island 02912
[52]University of Texas, Arlington, Texas 76019
[53]Texas A&M University, College Station, Texas 77843
[54]Rice University, Houston, Texas 77005

I. INTRODUCTION

At the Fermilab Tevatron, which operates at a center of mass energy of $\sqrt{s} = 1.8$ TeV, W and Z bosons are produced in high energy $\overline{p}p$ collisions. In addition to probing electroweak physics, the study of the production of W and Z bosons provides an avenue to explore QCD, the theory of strong interactions. The benefits of using intermediate vector bosons to study perturbative QCD are large momentum transfer, distinctive event signatures, low backgrounds, and a well understood electroweak vertex. In this paper we present the measurement of the angular distribution of electrons from W boson decays based on data taken by the DØ collider detector during the 1994–1995 Tevatron running period.

In the parton model, W and Z intermediate vector bosons are produced, at lowest order, in head-on collisions of $q\overline{q}$ constituents of the proton and antiproton, and cannot have any transverse momentum. This purely electroweak tree-level process is determined by the $(V - A)$ character of electroweak interactions and leads to a rather simple angular dependence of the cross section (measured by UA1 [1–3]):

$$\frac{d\sigma}{d(\cos\theta^*)} \propto (1 \pm \cos\theta^*)^2 \tag{1}$$

where θ^* is the lepton angle in the Collins-Soper rest frame [4] of the W boson in which the z-axis is defined as the bisector of the proton momentum and the negative of the antiproton momentum.

At large transverse momentum ($p_T > 20$ GeV), the cross section is dominated by the radiation of a single parton with large transverse momentum. Perturbative QCD [5,6] is therefore expected to be reliable in this regime. The additional gluon or quark jet in high p_T collisions alters the helicity-state of the W boson; a calculation to next-to-leading order in QCD leads to nine helicity amplitudes for the various contributing processes (see [7]). The cross section can be written in terms of the azimuthal and polar angles. Integrating over the azimuthal angle leads to:

$$\frac{d^3\sigma}{dq_T^2\, dy\, d\cos\theta^*} = C(1 + P(W)\alpha_1 \cos\theta^* + \alpha_2 \cos^2\theta^*) \tag{2}$$

where $P(W)$ is the polarization of the W boson. The angular parameters α_1 and α_2 are functions of the transverse momentum of the W boson, p_T^W, as shown in figure 1. In this paper we present a measurement of the parameter α_2 as a function of p_T^W. The angular parameter α_1 could not be measured by the DØ detector during Tevatron Run 1 because the lack of a magnetic field, for sign identification of electrons, makes it impossible to determine the polarization of the W boson. For Tevatron Run II, a central solenoid magnet will be installed, allowing for the measurement of both angular parameters.

The measurement of α_2 can serve as a probe for perturbative QCD independent of inclusive measurements. Since the transverse mass of the W boson is correlated with the decay angle of the lepton, QCD effects introduce a systematic shift to the W mass measurement at DØ , where a fit to the transverse mass distribution is used to determine the W mass. The shift, introduced by perturbative QCD, is $O(40$ MeV$)$ [8] for events with $p_T \leq 15$ GeV used in the mass measurement. In Run II, when the total error of the W mass will be reduced from the current 105 MeV [9,10] to an estimated 50 MeV for 1 fb^{-1} and to about 30 MeV for 10 fb^{-1} [11], a good understanding of this systematic shift is important.

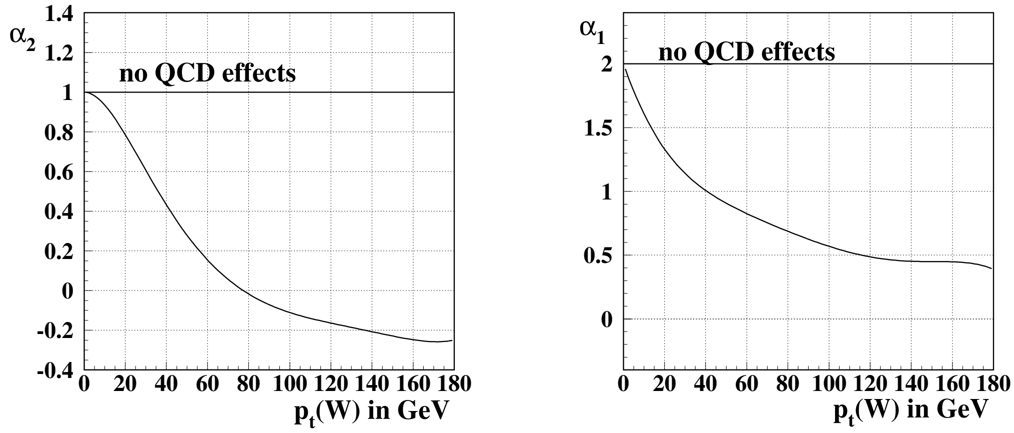

FIG. 1. The angular parameters α_2 (left) and α_1 (right) as a function of p_T^W.

II. EXPERIMENTAL METHOD

A. Extraction of the lepton angle

To directly measure the decay angle θ^* of the electron in the Collins-Soper frame, all momenta in the lab frame have to be known to perform the boost to this particular rest frame of the W Boson. This is not possible, however, since the longitudinal momentum of the neutrino cannot be measured. A solution to this problem is to use the correlation between $\cos\theta^*$ and the transverse W mass to infer $\cos\theta^*$ on a statistical basis. This is done using a Bayesian approach.

Figure 2 generated from Monte Carlo events that were run through a parameterized detector simulation (see [9] [12–14]) shows the correlation of the smeared W transverse mass and the true value of $\cos\theta^*$. By correlating the smeared transverse mass as it would be measured in the DØ detector and the true (unsmeared) value of $\cos\theta^*$, the Bayesian analysis described below will yield the unsmeared angular distribution. Note, however, that the angular distribution obtained this way is the distribution for accepted events which is different from the $1+P(W)\alpha_1\cos\theta^*+\alpha_2\cos^2\theta^*$ distribution expected for all events. Since the correlation between the angle and the transverse mass depends on the transverse momentum of the W boson, a separate correlation plot is used for each p_T bin. The correlation does not depend on the angular parameters α_1, and α_2, however, as can be seen from equation 3 [15]:

$$m_T^W = \frac{m_{e\nu}}{\sqrt{2}} \times \sqrt{2\sqrt{a_0 + a_1\gamma^2 + a_2\gamma^4} - 2(-\sin^2\theta^* + \gamma^2(1-\cos^2\phi^*\sin^2\theta^*)} \qquad (3)$$

where $m_{e\nu}$ is the invariant mass of the $e\nu$ system and the various parameters are defined as:

$$\gamma = \frac{p_T^W}{m_{e\nu}}$$
$$a_0 = \sin^4\theta^*$$
$$a_1 = 2\sin^2\theta^*(\sin^2\phi^* - \cos^2\phi^*\cos^2\theta^*)$$
$$a_2 = (1 - \cos^2\phi^*\cos^2\theta^*)^2$$

This equation provides the analytical expression for the dependence of the transverse mass on the angles θ^* and ϕ^*, where ϕ^* is the azimuthal angle in the Collins-Soper frame with respect to the x-axis: [15]. Note that in this analysis we integrate over ϕ^*.

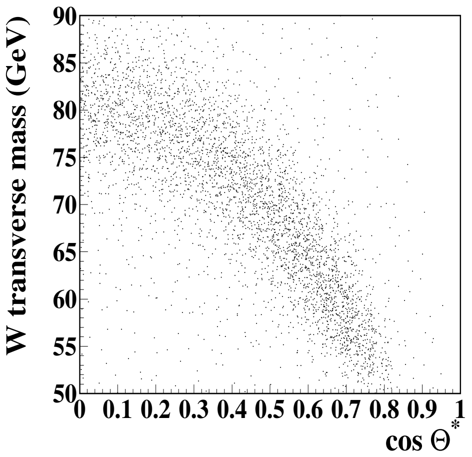

FIG. 2. Smeared W transverse mass versus true $\cos\theta^*$ for $p_T \leq 10$ GeV. Acceptance cuts are applied to this plot. This correlation plot is used to infer the $\cos\theta^*$ distribution from the measured m_T^W distribution.

To obtain an angular distribution from a measured transverse mass distribution, the transverse mass distribution has to be inverted using the following probability function:

$$f(\cos\theta^*|m_T) = \frac{g(m_T|\cos\theta^*)h(\cos\theta^*)}{\int g(m_T|\cos\theta^*)h(\cos\theta^*)d\cos\theta^*} \tag{4}$$

where:

- $g(m_T|\cos\theta^*)$ is the probability of measuring m_T given a certain $\cos\theta^*$ value (obtained from Monte Carlo) ;
- $h(\cos\theta^*)$ is the prior probability for $\cos\theta^*$: $(1+\cos^2\theta^*)$. It reflects all prior knowledge, i.e. the angular distribution in the absence of QCD effects;

- $f(\cos\theta^*|m_T)$ is the probability that an event with transverse mass m_T^W has a decay angle $\cos\theta^*$.

It is important to note that $g(m_T|\cos\theta^*) = \frac{N_{i,j,accepted}}{\sum_j N_{i,j,all}}$ where i is the bin number in m_T and j is the bin number in $\cos\theta^*$. The resulting $\cos\theta^*$ distribution is then the angular distribution for accepted events.

The angular distribution can now be inferred from the measured m_T^W distribution by integrating $f(\cos\theta^*|m_T)$ over m_T^W:

$$N_j = \sum_i^{all\, m_T\, bins} N_i^{m_T} f(\cos\theta_j^*|m_{Ti}) \tag{5}$$

where N_j is the number of events in $\cos\theta^*$ bin j.

To measure the angular parameter α_2 a series of $\cos\theta^*$ templates is generated from Monte Carlo in bins of p_T^W, each normalized to unity. Each of the templates is generated taking the transverse mass distribution from a high statistics Monte Carlo sample for a specific α_2 value and converting it into an angular distribution by means of the Bayesian method described previously. Detector effects are included by applying smearing, efficiency, and acceptance corrections in the Monte Carlo program. The angular distribution obtained from data is then compared to these templates to determine which value for α_2 fits best. Figure 3 shows a series of such templates for $p_T^W \leq 10$ GeV.

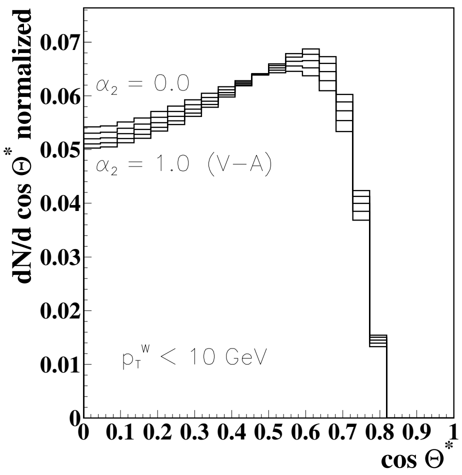

FIG. 3. Templates of the angular distribution for various α_2 values for $p_T^W \leq 10$ GeV. These templates are obtained from Monte Carlo after acceptance cuts have been applied which results in the drop-off at small angles.

B. Data Selection

The W sample has been selected from data taken during the 1994-95 run of the Tevatron, and corresponds to an integrated luminosity of 84.5 pb^{-1}.

The measurements of the W boson angular decay distribution used the decay mode $W \to e\nu$. Electrons were detected in hermetic, uranium/liquid-argon calorimeters with an energy resolution of about $15\%/\sqrt{E(\text{GeV})}$. The calorimeters have a granularity of $\Delta\eta \times \Delta\phi = 0.1 \times 0.1$, where η is the pseudorapidity and ϕ is the azimuthal angle. Electrons were accepted in the region $|\eta| < 1.1$ (central calorimeter). We assume that the transverse momentum of the neutrino is given by the calorimetric measurement of the missing transverse energy ($\not\!\!E_T$) in the event.

Electrons from W and Z boson decays tend to be isolated. Thus, we made the cut

$$\frac{E_{tot}(0.4) - E_{EM}(0.2)}{E_{EM}(0.2)} < 0.15,$$

where $E_{tot}(0.4)$ is the energy within $\Delta R < 0.4$ of the cluster centroid ($\Delta R = \sqrt{\Delta\eta^2 + \Delta\phi^2}$) and $E_{EM}(0.2)$ is the energy in the EM calorimeter within $\Delta R < 0.2$.

At trigger level, a single electron with E_T greater than 20 GeV was required. Off-line, a tighter requirement on the electron quality was introduced to reduce the background level from QCD dijet events, especially at high transverse momentum [16]. Electron identification was based on a likelihood technique. Candidates were first identified by finding isolated clusters of energy in the EM calorimeter with a matching track in the central detector. We then cut on a likelihood constructed from the following four variables: the χ^2 from a covariance matrix which measures the consistency of the calorimeter cluster shape with that of an electron shower; the electromagnetic energy fraction (defined as the ratio of the energy of the cluster found in the EM calorimeter to its total energy); a measure of the consistency between the track position and the cluster centroid; and the ionization dE/dx along the track. We require one central isolated electron and $\not\!\!E_T > 25$ GeV. The event is rejected if there is a second electron and the dielectron invariant mass lies in the range $75 - 105$ GeV. A total of 41173 central W candidates passed these cuts. A parametric Monte Carlo program [9] was used to simulate the DØ detector response and calculate the kinematic and geometric acceptance as a function of m_T and p_T. The detector resolutions used in the Monte Carlo were determined from data, and were parameterized as a function of energy and angle. The relative response of the hadronic and EM calorimeters was studied using the transverse momentum of the Z boson as measured by the p_T of the two electrons compared to the hadronic recoil system in the Z event.

C. Backgrounds

In order to use the transverse mass distribution of W Bosons to measure the angular distribution, the size of the backgrounds and their dependence on the two variables of interest here, transverse momentum and transverse mass, have to be estimated. The following sections describe how the four dominant backgrounds are calculated and how they depend on transverse mass and momentum.

1. QCD

QCD dijet events in which a jet is misidentified as an electron and the energy in the event is mismeasured which results in large missing transverse energy pose the largest overall background. The reason for this is the very large dijet cross section compared to the W cross section. This background is estimated from a data sample that is dominated by fake electrons which can be obtained by replacing the $\not\!\!E_T$ cut for W events with a complementary cut $\not\!\!E_T < 15$ GeV which selects events with fake electrons from multijet events with only a small contamination from real W events. The overall QCD background fraction is $f^W_{QCD} = (0.95\pm0.6)\%$ ($f^W_{QCD} = (0.77\pm0.6)\%$) without (with) a transverse mass cut of $50 < m^W_T < 90$ GeV imposed, which is the range used in the Bayesian analysis.

2. $Z \to ee$

Z events can look like W events if one electron is lost in an uninstrumented or under-instrumented region of the detector and the resulting energy imbalance amounts to large $\not\!\!E_T$. This background can only be estimated using Monte Carlo Z events. The number of such Z events present in the W sample is calculated by applying the W selection cuts to `HERWIG` [17] $Z \to ee$ events that were passed through a `GEANT` based simulation of the DØ detector and were overlaid with events from random $p\overline{p}$ crossings. The overall background fraction is$f^W_Z = 0.0091 \pm 0.0013$ for all p_T .

3. Top-Antitop

The top background is calculated in a similar way as the Z background from `HERWIG` $t\bar{t}$ events. The overall background fraction is$f^W_{top} = 0.0016 \pm 0.0005$ for all p_T .

4. $W \to \tau\nu$

$W \to \tau$ events where the τ subsequently decays into an electron and two neutrinos are indistinguishable from $W \to e\nu$ events. This background is included in the parameterized Monte Carlo described above: 2.22 % of the events are generated as τ's so that the plot correlating $\cos\theta^*$ and m^W_T simply takes these events into account.

Figure 4 shows the transverse mass distribution of $W \to e\nu$ candidates together with all backgrounds (excluding τ) in four p^W_T bins. All background rates are rather small. The background shapes shown here are fitted with heuristic functions and the errors on the fits are used to determine the systematic errors in the measurement of α_2 due to background subtraction.

D. The measurement of α_2

To obtain the angular distribution for W events from data, the transverse mass distribution is inverted according to the Bayesian method described in Section II A. Figure 5 shows

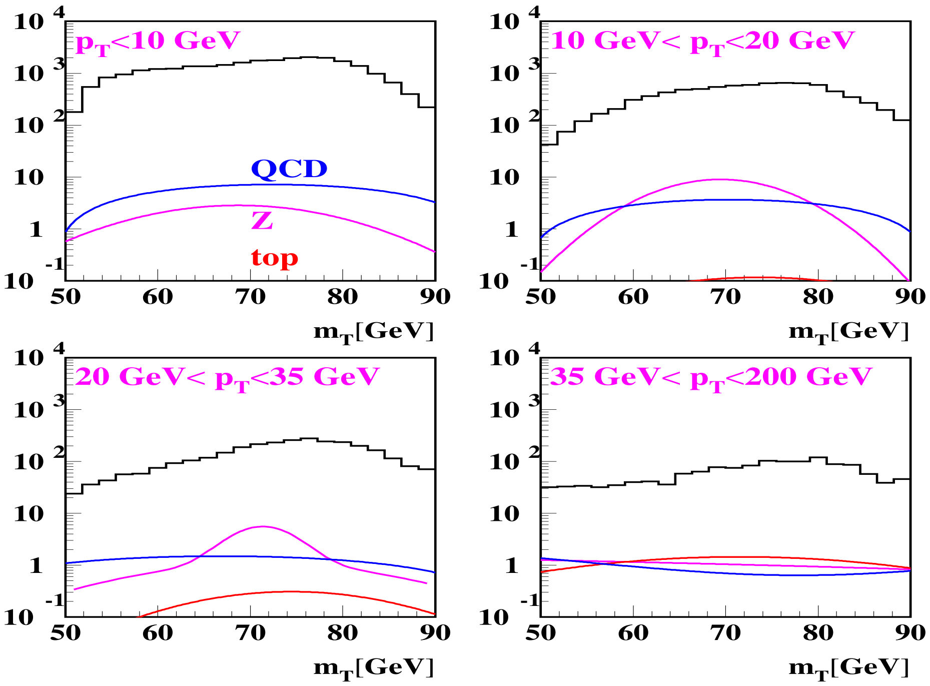

FIG. 4. Summary of all backgrounds in four p_T bins.

the background subtracted transverse mass distributions for the four p_T bins used in this analysis. The χ^2-values per degree of freedom are 1.67, 1.77, 1.02, and 1.10, respectively, in order of increasing p_T .

To extract the angular parameter α_2 from the angular distribution obtained by inverting the transverse mass distribution a log-likelihood method is used,

$$\ln \mathcal{L} = \sum_{i}^{all\ \cos\theta^*\ bins} n_i \ln p_i \tag{6}$$

where p_i is the normalized population of a $\cos\theta^*$ bin for one of the Monte Carlo templates and n_i is the population of the same bin in the angular distribution obtained from data. The statistical errors for α_2 are taken at the points where $\ln \mathcal{L}$ drops by 0.5 units.

In figure 6 the angular distributions obtained from data are compared to the Monte-Carlo templates that fit best. In figure 7 the log-likelihood distributions for α_2 are shown in the four p_T ranges. To estimate the sensitivity of this experiment the χ^2 of the α_2 distribution is calculated with respect to the next-to-leading order QCD prediction and with respect to $(V-A)$ theory in the absence of QCD. The χ^2 with respect to the QCD prediction is 0.9/4 dof which corresponds to a probability of 93%. The χ^2 with respect to the no-QCD prediction is 7.0/4 dof which corresponds to 14%. Using the odds-ratio technique, the next-to-leading order QCD calculation is found to be preferred by $\approx 2\sigma$ over the calculation in the absence of QCD. The results of this measurement, including the dominant sources of error, are summarized in figure 8 and table I. The systematic errors are estimated by varying the relevant parameter (like background shape, overall background rate, or modeling parameters) in the Monte Carlo by their errors and rerunning the analysis program resulting in a varied angular parameter α_2.

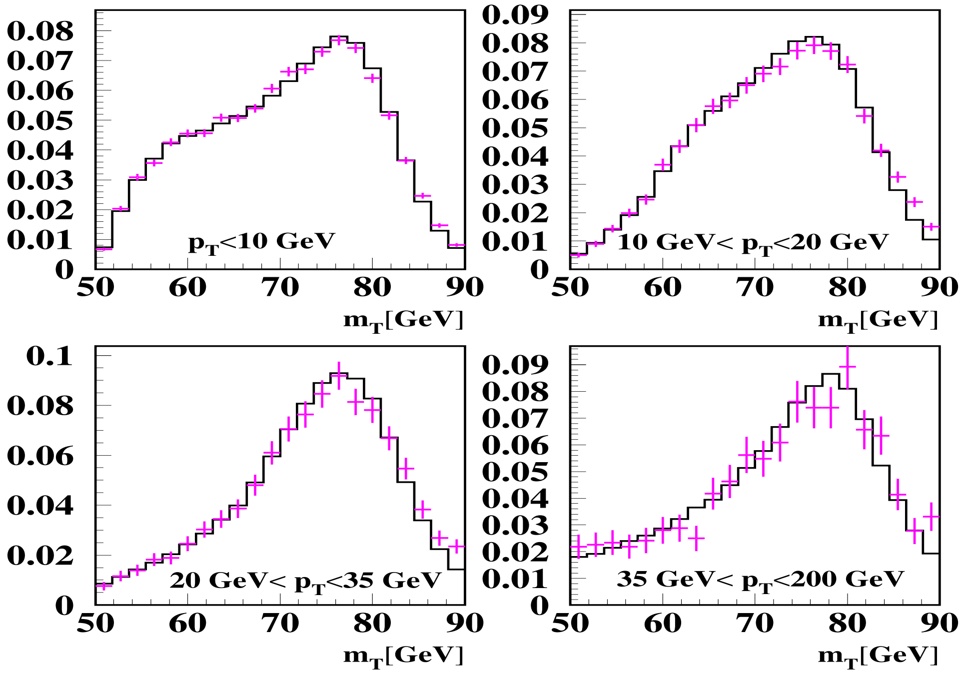

FIG. 5. Background subtracted transverse mass distributions(crosses) in four p_T bins compared to Monte Carlo predictions (lines). (DØ preliminary)

p_T	$0 \leq p_T \leq 10$	$10 \leq p_T \leq 20$	$20 \leq p_T \leq 35$	$35 \leq p_T \leq 200$
α_2	1.07 ± 0.12	0.81 ± 0.23	0.52 ± 0.35	0.19 ± 0.40
α_2, *predicted*	0.99	0.90	0.69	0.23
mean p_T	4.4	12.6	25.7	53.6
error QCD	±0.022	±0.048	±0.086	±0.069
error QCD shape	±0.035	±0.004	±0.026	±0.008
error Z	±0.002	±0.01	±0.01	±0.04
error Z shape	±0.00	±0.01	±0.01	±0.02
error top	±0.0005	±0.0002	±0.001	±0.008
error hadronic response	±0.013	±0.00	±0.06	±0.07
error hadronic recoil model	±0.04	±0.09	±0.10	±0.10

TABLE I. Central values and statistical errors for α_2 and systematic errors due to backgrounds and the hadronic energy scale and resolution.

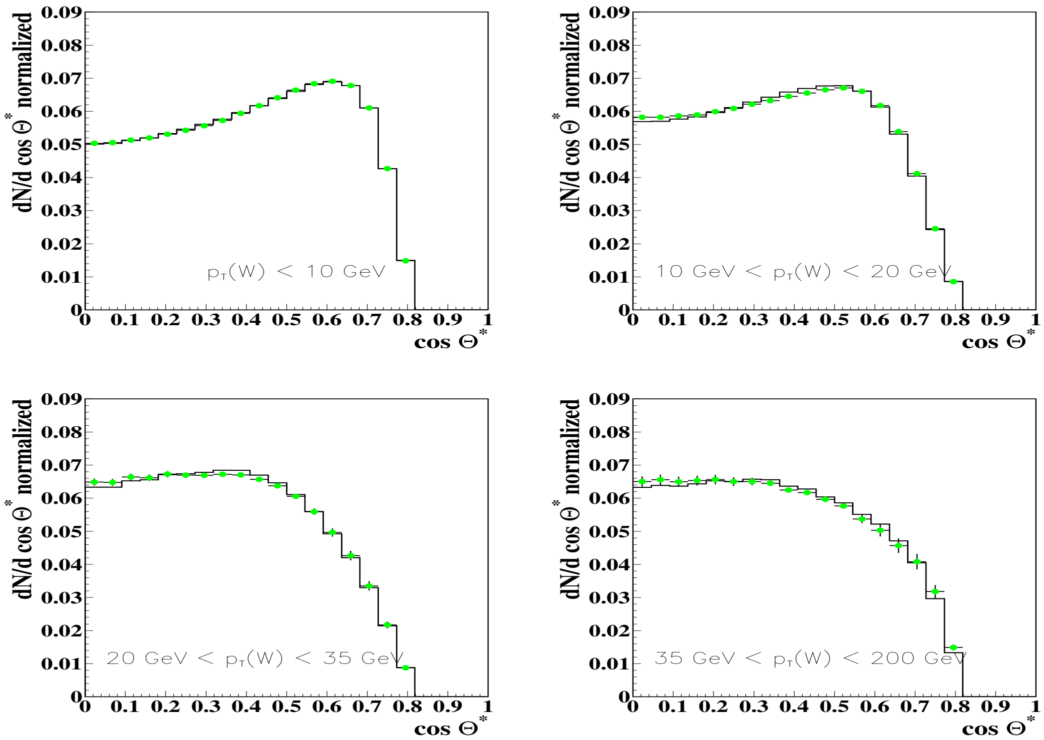

FIG. 6. Angular distributions for data (crosses) compared to Monte Carlo templates (lines) for four different p_T bins. (DØ preliminary)

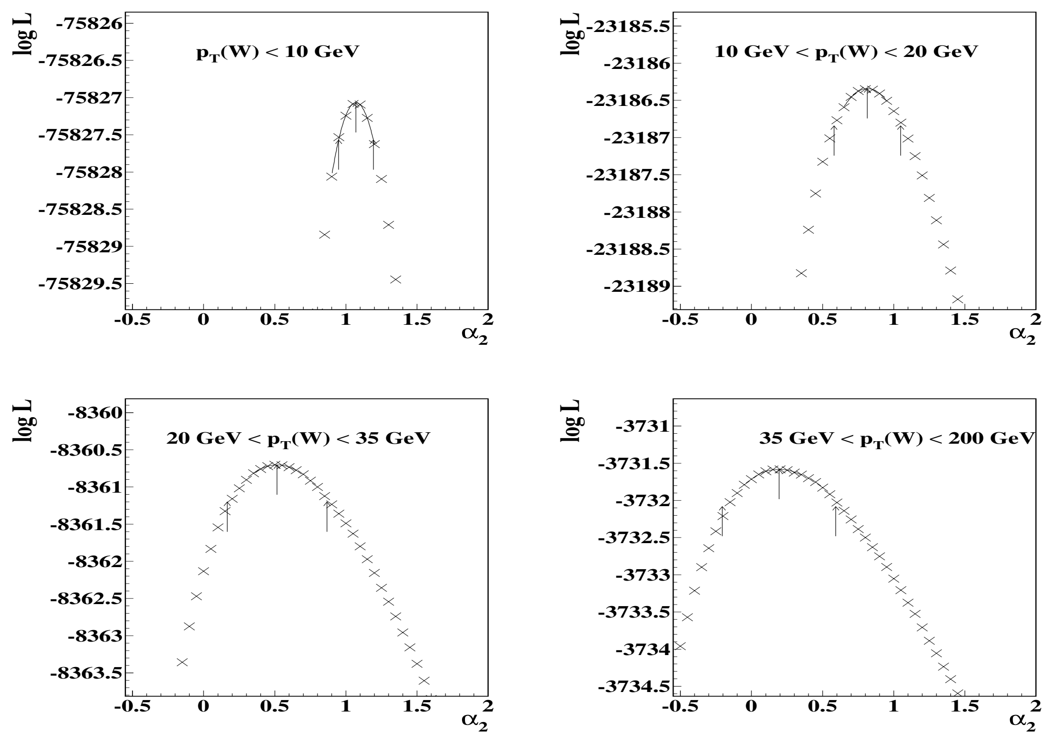

FIG. 7. Log likelihood functions for four different p_T bins.

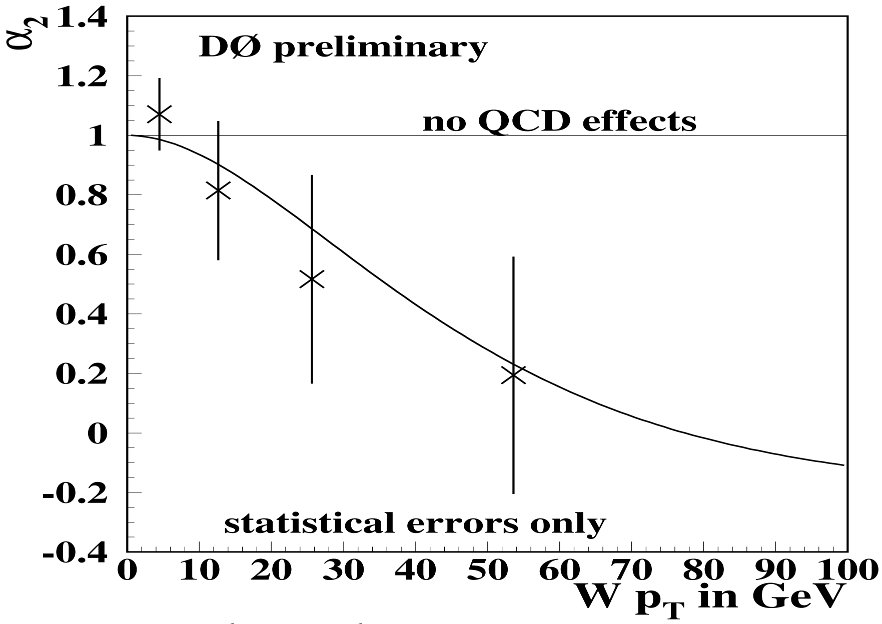

FIG. 8. Measured α_2 as a function of p_T and its statistical errors compared to next-to-leading order QCD calculation by Mirkes (curve) and calculation in the absence of QCD (horizontal line).

III. CONCLUSIONS

Using data taken with the DØ detector during the 1994–1995 Tevatron collider run, we have presented the measurement of the angular distribution of decay electrons from W boson events. A next-to-leading order QCD calculation is preferred by $\approx 2\sigma$ over a calculation where no QCD effects are taken into account.

IV. ACKNOWLEDGEMENTS

We thank the Fermilab and collaborating institution staffs for contributions to this work and acknowledge support from the Department of Energy and National Science Foundation (USA), Commissariat à L'Energie Atomique (France), Ministry for Science and Technology and Ministry for Atomic Energy (Russia), CAPES and CNPq (Brazil), Departments of Atomic Energy and Science and Education (India), Colciencias (Colombia), CONACyT (Mexico), Ministry of Education and KOSEF (Korea), and CONICET and UBACyT (Argentina).

REFERENCES

[1] G, Arnison et al. (UA1 collaboration), Phys.Lett. **166** B:484,(1986)

[2] E.Locci. Proc. 8th European Symp. on Nucleon-Antinucleon Interactions, Thessaloniki,(1986)

[3] C. Albajar et al. (UA1 collaboration), Z,Phys. C **44:15**,(1989)

[4] J.C. Collins, D.E. Soper. Phys. Rev. D **16**,2219, (1977)

[5] P. B. Arnold and M. H. Reno, Nucl. Phys. **B319**, 37 (1989); R. J. Gonsalves, J. Pawlowski, and C-F. Wai, Phys. Rev. D **40**, 2245 (1989).

[6] P. B. Arnold and R. Kauffman, Nucl. Phys. **B349**, 381 (1991).

[7] E. Mirkes. Nuclear Physics, **B387** 3 (1992)

[8] DØ Internal note 3198

[9] B. Abbott et al. (DØ collaboration), Phys. Rev. D **58**, 092003 (1998)

[10] B. Abbott et al. (DØ collaboration), Phys. Rev. Lett. **80**, 3000 (1998).

[11] TEV 2000, Fermilab Pub 96/082

[12] Eric Flattum, Ph.D. thesis, Michigan State University, 1996 (unpublished)

[13] I. Adam, Ph.D. thesis, Columbia University, 1997 (unpublished), Nevis Report #294

[14] B. Abbott et al. (DØ collaboration), Physics Rev. Lett. **80** 5498 (1998)

[15] M. I. Martin. 1994, thesis (unpublished)

[16] B. Abbott et al. (DØ collaboration), "Measurement of the Transverse Momentum Distribution of W and Z Bosons in $\overline{p}\,p$ Collisions at $\sqrt{s} = 1.8$ TeV ", paper submitted to the International Europhysics Conference on High Energy Physics: EPS99; Tampere, Finland July, 1999

[17] G. Marchesini et al., Comput. Phys. Commun. **67**, 465 (1992)